Iterative CT reconstruction with correction for known rigid motion.

Johan Nuyts[1], Jung-ha Kim[2], Roger Fulton[2]

***Abstract*—In PET/CT brain imaging, correction for motion may be needed, in particular for children and psychiatric patients. Motion is more likely to occur in the lengthy PET measurement, but also during the short CT acquisition patient motion is possible. Rigid motion of the head can be measured independently from the PET/CT system with optical devices. In this paper, we propose a method and some preliminary simulation results for iterative CT reconstruction with correction for known rigid motion. We implemented an iterative algorithm for fully 3D reconstruction from helical CT scans. The motion of the head is incorporated in the system matrix as a view-dependent motion of the CT-system. The first simulation results indicate that some motion patterns may produce loss of essential data. This loss precludes exact reconstruction and results in artifacts in the reconstruction, even when motion is taken into account. However, by reducing the pitch during acquisition, the same motion pattern no longer caused artifacts in the motion corrected image.**

***Index Terms*—CT, motion correction, reconstruction**

I. Introduction

For PET brain imaging with current PET/CT systems, usually a low dose CT measurement is acquired for attenuation correction of the PET images. Because of the long scan duration, patients frequently move during PET scanning, which causes motion artifacts in the reconstructed images. With optical devices, this motion can be measured, and the resulting information can be used to compensate for the time dependent pose of the head during PET reconstruction [1], [2]. When such an optical device is installed for the PET acquisition, it can be used to detect the (less likely) patient motions during the fast CT acquisition as well. Here, we evaluate an iterative maximum likelihood algorithm that is adapted to compensate for the measured motion. It is assumed that the motion is rigid, and therefore the problem at hand is simpler than the problem of correcting for breathing motion that occurs during slow cone beam CT scanning [3], [4]. Instead of modelling the motion as a change of the object to be imaged, we can assume a stationary object imaged by the rigid CT-system, and incorporate the motion into the orbit of the CT-system.

In the following section, we first present the maximum likelihood algorithm implemented for 3D reconstruction from helical CT acquisitions with a clinical scanner. The algorithm without motion correction is illustrated on a clinical data set. Then, a few preliminary simulation experiments are presented to evaluate the artifacts caused by motion, when that motion is or is not taken into account during reconstruction. Comparison of simulations with a pitch of 2 and a pitch of 0.5 indicate that motion correction is more effective for CT-acquisitions at low pitch.

[1]Nuclear Medicine, K.U.Leuven, U.Z.Gasthuisberg, Leuven, Belgium
[2]School of Physics - The University of Sydney and Medical Physics - Westmead Hospital, Sydney, Australia
Corresponding author: JN, Johan.Nuyts@uz.kuleuven.be

II. Methods

We have implemented a version of the so called MLTR algorithm [5], for reconstruction from data acquired on a clinical CT-scanner. This algorithm maximises the likelihood $L(\mu)$, which for the case where detector blurring and scatter are ignored, is given by

$$L(\mu) = \sum_i y_i \ln \bar{y}_i - \bar{y}_i \quad (1)$$

$$\bar{y}_i = b_i e^{-\sum_j l_{ij}\mu_j}, \quad (2)$$

where μ_j is the linear attenuation coefficient at voxel j, y_i is the transmission value measured at detector i, and l_{ij} is the intersection length of projection line i with voxel j. The algorithm can be written as

$$\mu_j^{\text{new}} = \mu_j + \frac{\sum_i l_{ij}(\bar{y}_i - y_i)}{\sum_i (l_{ij}\bar{y}_i \sum_k l_{ik})}. \quad (3)$$

A derivation is given in appendix A. This algorithm is also a special case of the class of algorithms derived in [6]. It is straightforward to accelerate MLTR with subsets [7], by restricting the backprojections in the numerator and denominator to the current subset in every subiteration.

The projector/backprojector was implemented using the distance driven approach [8]. When motion is included, the detector and source are translated and rotated, and the (back)projection is computed using this moved CT-system. A different rotation and translation can be assigned to each individual view (where 'view' denotes the set of simultaneously acquired detector values at a particular position in the helical orbit). The detector motion is the inverse of the known patient motion. This method is analogous to one previously described for motion correction in SPECT [9], [10]. An alternative approach would be to move the image instead of the CT, as was done in [11] for SPECT, but because of the high number of views in CT, moving the CT should be more efficient.

Fig. 1 compares the MLTR reconstruction and the reconstruction using the analytic algorithm from the manufacturer, for a patient CT scan acquired on a Siemens Biograph 16 PET/CT system. The scan contained 9918 views with 1160 views per rotation, a pitch of 2 and a collimation of 16 $\times$ 0.75 mm were used. For this test, MLTR was applied with 10 iterations and 290 subsets (i.e. each subset contained 4 views per rotation).

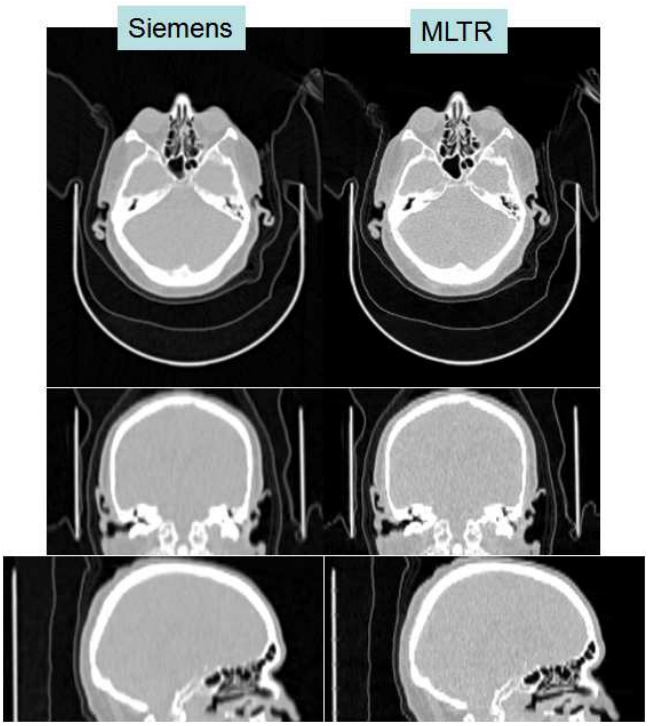

Fig. 1. Reconstructions from a clinical CT-scan. Left: the clinical reconstruction obtained with the commercial software. Right: the reconstruction obtained with MLTR.

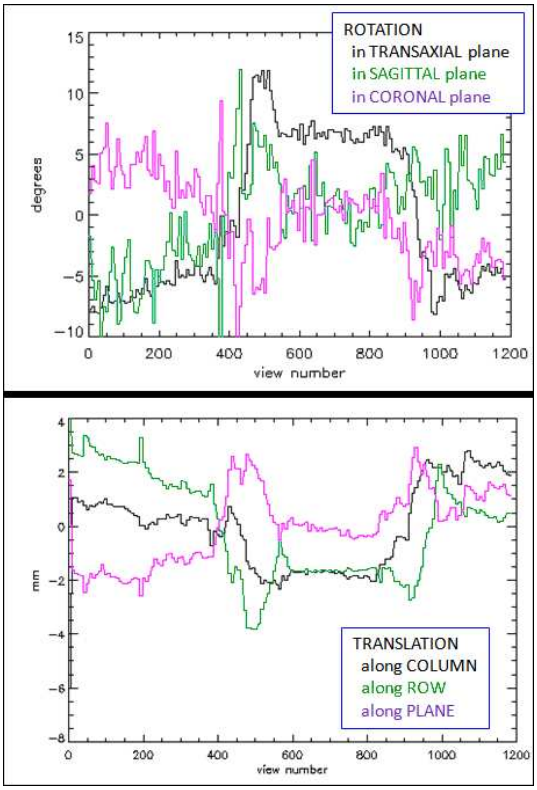

Fig. 2. The three rotations (in degrees) and translations (in mm) obtained from the small animal experiment.

The good agreement validates the (back)projector used in MLTR. The MLTR-reconstruction is slightly sharper and noisier, because it deblurs the unavoidable blurring from the projector.

III. Simulation Experiments

A. Helical scan with motion, pitch = 2

For a first experiment with somewhat realistic object motion, a 5 seconds extract from the motion record from an awake rat during a microPET brain scan was used [2]. The three original rotations and translations are shown in figure 2. The rotations were used without change, the translations were multiplied by 3 to obtain reasonable values for human imaging.

A 3D phantom composed of ellipsoids was used as the object, and helical scans were simulated. During simulation, the motion was created by rotating and translating the voxelized object using linear interpolation. When a fixed translation and rotation was applied and corrected for during reconstruction, no artifacts were observed. This indicates that the mismatch between simulated motion (movement of the object with linear interpolation) and the motion during reconstruction (movement of the detector with distance driven interpolation) does not cause noticeable artifacts. Hopefully, the same will be true for the mismatch between true patient motion and the proposed motion model.

The object was scanned using a standard helical orbit with pitch equal to 2. The motion was interpolated to give it the same duration as the entire helical scan. As shown in fig. 3, the motion caused considerable artifacts, which were strongly reduced with motion correction. However, some

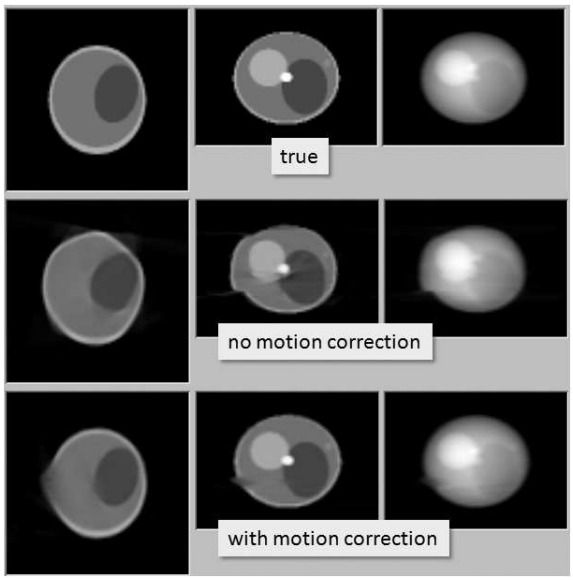

Fig. 3. Transaxial slice, coronal slice and projection image of 1) the true image, 2) the reconstruction without motion correction and 3) the reconstruction with motion correction, for a simulated CT scan with pitch = 2.

artifacts persisted after motion correction. When the MLTR reconstruction with motion correction was started from the true solution, the algorithm did not change the initial image. This indicates that (some of) the motions cause loss of data, and that the resulting missing data problem does not have a unique solution.

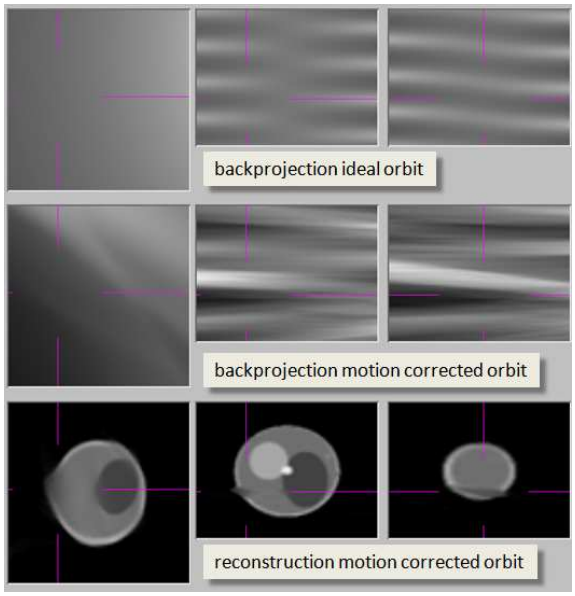

Fig. 4. Transaxial, coronal and sagittal slices of 1) backprojection of a uniform sinogram for the ideal helical orbit, 2) the same for the motion corrected orbit and 3) the reconstruction with motion correction. Helical orbit with pitch = 2.

This is further illustrated in fig 4, where the reconstruction with motion correction is shown together with the backprojection of a uniform sinogram (all sinogram pixels set to 1). For the ideal orbit, the backprojection fills the reconstruction volume well. However, for the motion corrected orbit, parts of the volume are very poorly sampled by projection lines, which results in missing data. The persistent artifacts show up in regions that are poorly sampled during backprojection.

The six motion components were also applied one at a time, and reconstructions with motion compensation were computed. This revealed that significant reconstruction errors occurred for only two of the motion components: translation in the axial direction, and rotation in the coronal plane. It was verified that the combination of the four other components did not produce noticeable artifacts after reconstruction with motion compensation.

B. Helical scan with motion, pitch = 0.5

To increase the robustness to patient motion, a scan with a reduced pitch of 0.5 was simulated. Because such a scan would take more time, the motion pattern was repeated three times during the scan. In absence of motion, a low pitch scan yields redundant data, and such redundancy should increase the robustness against local loss of information. As shown in fig 5 this was indeed the case, and for this motion pattern an artifact free reconstruction was obtained from MLTR with motion correction. Note that there are still regions that are poorly sampled. However, these samples now contain more information, because they are produced by projection lines with more variation in the acquisition angle.

IV. Discussion and Conclusion

A fully 3D maximum likelihood reconstruction for helical CT was extended to include view-dependent motion, enabling correction for known rigid patient motion. Experiments indicate that some motions may cause loss of essential information, and as a result, artifacts are seen even after motion correction. For this experiment, these residual artifacts were mainly caused by translation along the rotation axis and rotation in the coronal plane. In contrast to transaxial translations, a translation along the rotation axis tends to shift part of the object (temporarily) out of the field of view, and therefore may lead to loss of essential angular sampling. Rotations in the coronal or sagittal plane can also move parts of the object out of the field of view. It is not yet clear why in this experiment, the rotation in the coronal plane caused more problems than the one in the sagittal plane, since the motions are of the same order (fig 2). A possible explanation is that the coronal rotation curve has more abrupt changes than the sagittal one. This is better seen in fig 6, which shows smoothed versions of the three rotation curves from fig 2). We assume that the coronal rotations yielded more residual artifacts, because sudden rotations cause more loss of information than slow rotations.

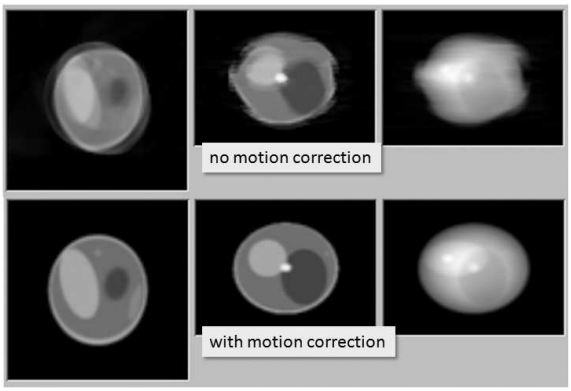

Fig. 5. Transaxial, coronal and projection images of 1) MLTR reconstruction without motion correction 2) MLTR reconstruction with motion correction for a helical orbit with pitch = 0.5.

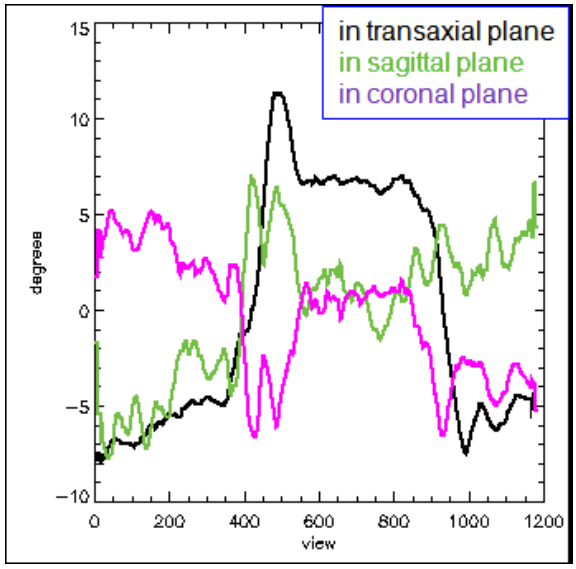

Fig. 6. The three rotation components of fig 2, after smoothing for better visualisation.

The robustness to patient motion can be improved by using helical orbits with low pitch. In the simulation presented here, all artifacts were eliminated if the scan was done with a pitch of 0.5. Reducing the pitch tends to increase the radiation dose. However, our current minimal dose brain CT protocol corresponds to an effective dose of 0.04 mSv. Therefore, even with a moderate dose increase the CT dose would still be very small compared to the PET related dose (typically a few mSv). To optimise the acquisition protocol, more studies with true patient motion data should be carried out, and the results should be validated with measured phantom data.

An alternative way to increase the robustness would be to introduce some regularization. For example, it has been shown that a regularization based on minimum total variation [12] improves the reconstruction in limited angle tomography. If the scan is only acquired for attenuation correction, strong regularization would be acceptable.

In both CT and SPECT, projection views are acquired sequentially by rotating the detector during acquisition. We show here that the expedient, originally proposed for SPECT, of performing fully 3D reconstruction from views that have been repositioned and reorientated in response to observed patient motion, is also applicable in CT. However axial bed motion in spiral CT is an additional complication not encountered in SPECT that affects data sufficiency. In both modalities it must be assumed that no motion occurs while an individual projection view is being acquired. This assumption appears reasonable in CT as each projection view is acquired over a very short time interval.

In these experiments, we have ignored the patient bed and/or head holder, which remains stationary while the patient moves. If ignoring the head holder would cause only limited and localised artifacts, it could simply be erased in the final reconstruction, and instead a correct image of the head holder could be inserted, since its position, shape and attenuation are known a priori. However, for large patient movements and head holders with significant attenuation, it may be necessary to take the stationary head holder into account during reconstruction.

APPENDIX A
A DERIVATION OF THE MLTR ALGORITHM

Suppose that the current reconstruction is μ, and that in each iteration, the new reconstruction $\mu+\Delta\mu$ is obtained by adding a fairly small update $\Delta\mu$. It is assumed that at each iteration, the likelihood can be well approximated as a truncated series expansion:

$$\begin{aligned} L(\mu+\Delta\mu) &\simeq T_1(\mu,\Delta\mu) \\ &= L(\mu)+\sum_j \frac{\partial L}{\partial \mu_j}\Delta\mu_j + \frac{1}{2}\sum_{j,k}\frac{\partial^2 L}{\partial\mu_j\partial\mu_k}\Delta\mu_j\Delta\mu_k \end{aligned} \quad (4)$$

where the derivatives are evaluated in the current reconstruction image μ. Because the second derivatives are negative, and because $2\Delta\mu_j\Delta\mu_k \le \Delta\mu_j^2+\Delta\mu_k^2$ we can introduce a surrogate function T_2 such that we have

$$\begin{aligned} T_1(\mu,\Delta\mu) &\ge T_2(\mu,\Delta\mu) \\ &= L(\mu)+\sum_j \frac{\partial L}{\partial \mu_j}\Delta\mu_j + \frac{1}{2}\sum_{j,k}\frac{\partial^2 L}{\partial\mu_j\partial\mu_k}\Delta\mu_j^2. \quad (5) \\ T_1(\mu,0) &= T_2(\mu,0) \quad (6) \end{aligned}$$

T_2 is easily maximised because all terms in $\Delta\mu_j$ are separated. We obtain the update expression

$$\Delta\mu_j = -\frac{\partial L}{\partial\mu_j}\Big/\sum_k \frac{\partial^2 L}{\partial\mu_j\partial\mu_k} \quad (7)$$

This update maximises $T_2(\mu,\Delta\mu)$, and by (6) and (5), it also increases $T_1(\mu,\Delta\mu)$. To the extent that approximation (5) applies, also the likelihood $L(\mu+\Delta\mu)$ will increase. Evaluating (7) yields (3).

ACKNOWLEDGEMENT

The authors would like to thank Karl Stierstorfer from Siemens Erlangen for his help with defining the CT-projector, and Andre Kyme, a PhD student in the School of Physics at the University of Sydney, for kindly providing the rat motion data.

REFERENCES

[1] PM Bloomfield, TJ Spinks, J Reed, L Schnorr, AM Westrip, L Livieratos, R Fulton, T Jones, "The design and implementation of a motion correction scheme for neurological PET". *Phys Med Biol* 2003; 48: 959-978

[2] AZ Kyme, VW Zhou, SR Meikle, RR Fulton. "Real-time 3D motion tracking for small animal brain PET". *Phys Med Biol* 2008; 53: 2651-2666.

[3] T Li, E Schreibmann, Y Yang, L Xing. "Motion correction for improved target localization with on-board cone-beam computed tomography". *Phys Med Biol* 2006; 51: 253-267.

[4] S Rit, D Sarrut, L Desbat. "Comparison of Analytic and Algebraic Methods for Motion-Compensated Cone-Beam CT Reconstruction of the Thorax". *IEEE Trans Med Imaging*, 2009; 28: 1513-1525.

[5] J. Nuyts, B. De Man, P. Dupont, M. Defrise, P. Suetens, L. Mortelmans. "Iterative reconstruction for helical CT: a simulation study." *Phys Med Biol*, 1998; 43: 729-737.

[6] JA Fessler, EP Ficaro, NH Clinthorne, K Lange. "Grouped-Coordinate Ascent Algorithms for Penalized-Likelihood Transmission Image Reconstruction". *IEEE Trans Med Imaging* 1997; 16: 166-175.

[7] MH Hudson, RS Larkin. "Accelerated image reconstruction using ordered subsets of projection data". *IEEE Trans Med Imaging*, 1994, 13: 601-609.

[8] B De Man, S Basu. "Distance-driven projection and backprojection in three dimensions". *Phys Med Biol* 2004; 49: 2463-2475.

[9] RR Fulton, BF Hutton, M Braun, B Ardekani, R Larkin. "Use of 3D reconstruction to correct for patient motion in SPECT". *Phys Med Biol* 1994; 39: 563-574.

[10] RR Fulton, S Eberl, SR Meikle, BF Hutton, M Braun. "A practical 3D tomographic method for correcting patient head motion in clinical SPECT". *IEEE Tran Nucl Sci* 1999; 46(3): 667-672.

[11] B Feng, HC Gifford, RD Beach, G Boening, MA Gennert, MA King. "Use of three-dimensional Gaussian interpolation in the projector/backprojector pair of iterative reconstruction for compensation of known rigid-body motion in SPECT". *IEEE Trans Med Imaging* 2006; 25 (7): 838-844

[12] M Persson, D Bone, H Elmqvist. "Total variation norm for three-dimensional iterative reconstruction in limited view angle tomography". *Phys Med Biol*, 2001; 46 (3): 853-866.